ACS Catalysis

Research Article

pubs.acs.org/acscatalysis

Polyelectrolyte Doped Hollow Nanofibers for Positional Assembly of Bienzyme System for Cascade Reaction at O/W Interface

Xiaoyuan Ji,[†,‡] Zhiguo Su,[†,∥] Ping Wang,[†,§] Guanghui Ma,[†] and Songping Zhang*[,†,∥]

[†]National Key Laboratory of Biochemical Engineering Institute of Process Engineering, Chinese Academy of Sciences, Beijing 100190, China

[‡]University of Chinese Academy of Sciences, Beijing, 100049, P.R. China

[§]Department of Bioproducts and Biosystems Engineering and Biotechnology Institute University of Minnesota, St. Paul, Minnesota 55108, United States

[∥]Collaborative Innovation Center of Chemical Science and Engineering (Tianjin), Tianjin, 300072, P.R. China

ABSTRACT: Cationic polyelectrolyte doped hollow nanofibers prepared via facial coaxial electrospinning technology have been used for positional assembly of two enzymes, glucose oxidase (GOD) and *Candida antactica* lipase B (CALB), at two different positions, namely, in their lumen and on their surface. Therefore, the result is four combinations, including lumen (GOD+CALB), surface (GOD+CALB), surface (GOD)-lumen (CALB), and lumen (GOD)-surface (CALB). Surface attachment of enzymes was achieved by layer-by-layer (LbL) technology, which is based on the ion-exchange interactions between oppositely charged enzymes and polyelectrolyte that was doped in hollow nanofibers; whereas placing enzymes inside the lumen of hollow nanofibers was realized by in situ encapsulation during coelectrospinning. The hollow nanofibers-based bienzyme systems were used for a cascade reaction in an oil-aqueous biphasic system, in which glucose was oxidized by GOD to generate H_2O_2, which was used as substrate and oxidant for CALB-catalyzed epoxidation of oleic acid in the second step. The bienzyme nanofibers membrane was found to float spontaneously at the O/W interface, which is advantageous to biphasic biocatalysis. Assembly strategies of the two enzymes affect their biocatalytic efficiency significantly by influencing the utilization efficiency of H_2O_2 in the reaction process. The highest reaction rate was attained by lumen (GOD)-surface (CALB), corresponding to 114.45 times enhancement as compared to that of the free bienzyme system.

KEYWORDS: *cascade reactions, coaxial electrospinning, polyelectrolyte, hollow nanofibers, positional assembly*

1. INTRODUCTION

Thousands of different chemical reactions catalyzed by various multienzyme systems take place inside living cells to support cellular growth and survival. Although these in vivo multienzyme systems are complicated and diverse, they all have excellent chemo-, regio-, stereoselectivity and high efficiency. With the development of industrial biotechnology, constructing and applying multienzyme cascade reactions in vitro is on the verge of rapid growth from both academic and industrial aspects, particularly in biomedical, biosensor, and biotransformation fields.[1−3] In contrast to the microbial-catalyzed multistep metabolic process which is usually less efficient due to formation and degradation of intermediates and unexpected side products, as well as the consumption of nutrient substance for supporting cell group, the synthetic route of in vivo multienzyme system can be flexibly designed and optimized.[1−6] One example is the production of H_2 from xylose, one mole of xylose can generate 9.6 mol of H_2 by using a synthetic enzyme cascade involving 13 enzymes and cofactors in a cell-free system, while only 3.33 mol of H_2 can be generated at most by using microorganisms.[7−9]

Cell-free multienzyme biotransformation sounds attractive. However, for the free enzymes in environments slightly outside of the biocompatible regimes, they are relatively unstable and cannot be efficiently recovered and reused, and as a consequence, the advantages of free mutlienzymes versus whole cells may be reduced. To accomplish their recycling in practical application, immobilization of enzymes is an effective approach, and in some circumstances, well-designed immobilization may even improve many of other important features of the enzyme, like activities, stabilities, specificity, and so forth.[10−16] For multienzyme system construction, the selectivity and high efficiency is usually highly dependent on the precisely controlled location of each enzyme, which is realized in vivo by the high-degree compartmentation of the biological cells.[17−21] The compartmentalization is therefore considered as one of the most crucial techniques that cells adopt to enable a high level of control over bio/chemical processes, in which numerous

Received: September 13, 2014
Revised: November 7, 2014
Published: November 10, 2014

   dx.doi.org/10.1021/cs501383j | ACS Catal. 2014, 4, 4548−4559

Scheme 1. Schematic Illustrations of the Setup for Co-Axial Electrospinning and Positional Assembly of GOD/CALB Bienzyme Based on PAH Doped PU Hollow Nanofibers

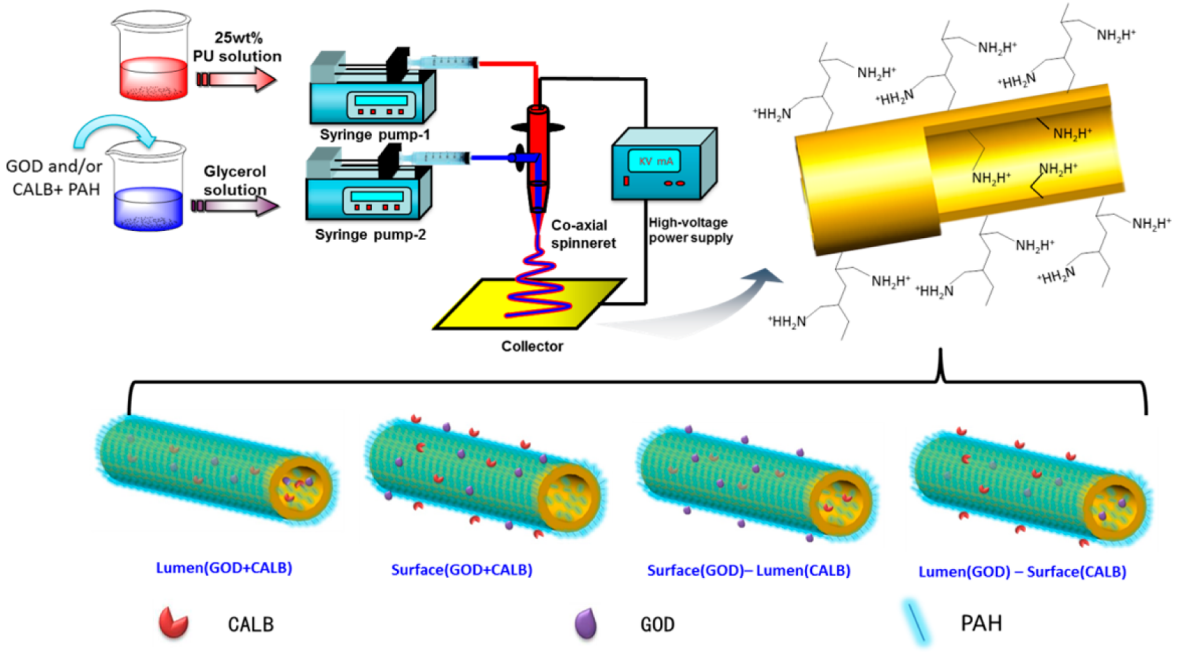

multistep reactions take place simultaneously with unsurpassed efficiency and specificity,[17−21] at the same time, providing a solid scaffold for precise positional assembly of multienzyme system and spatial isolation of enzymes so that any possible negative interferences between different enzymes can be avoided.[18,22,23] Due to the complexity of the in vivo multienzyme system, how to biomimetically construct an immobilized multienzyme system that can efficiently perform multistep biotransformation has always been the most important and challenging task from both biology and materialogy aspects.[24−28]

Nowadays, many efforts have been devoted to mimic this natural concept of enzyme assembly by encapsulation.[19,21,29,30] According to the structure of compartmentation, current artificial designs for positional assembly of enzymes can be classified into single-chamber microcapsule (liposome and polymersome),[18,31−37] multichambers microcapsule,[38,39] shell-in-shell microcapsule[40−42] and polymersomes within a polymersome.[43,44] From an industrial standpoint, however, most of these compartmental encapsulation of multienzyme systems have limitations owing to the complicated and nonbiofriendly preparation process, enzyme deactivation upon direct contact with organic solvents used to dissolve the template, low loading capacity, difficulty in reuse, and so on. On the other hand, systematic investigations on the influence of different positional assembly on the efficiency of a multienzyme system have been deficient.

Advances in electrospinning techniques for fabricating nanofibers with a multilever interior structure for the formation of continuous nonwoven membranes inspired us to redesign the natural concept of enzyme assembly and encapsulation for multienzyme biotransformation.[45−51] Recently, electrospinning of two immiscible liquids through a coaxial, two-capillary spinneret, which was proposed by Loscertales et al.,[52,53] has been successfully adopted in our lab to directly fabricate hollow nanofibers-based multienzyme system for bile acid detection, in which two oxidoreductases and shared coenzymes were in situ encapsulated inside the nanochamber of the hollow nanofibers.[54] Compared to the previously reported assembled multienzyme systems which take the form of microcapsules, several advantages of hollow nanofibers-based multienzyme system have been proven as follows: specially designed two-capillary spinneret will prevent the bioactive molecules from contacting with the organic solvent; the in situ encapsulation process ensures nearly 100% loading efficiency for expensive enzymes; the confinement of the multienzyme system inside the nanoscaled compartments enhances the enzymes stability; the woven-membrane nanofibers enable easy recycling and operation.[54]

The polyelectrolyte layer-by-layer (LbL) technique, which is usually based on the ion-exchange interactions between oppositely charged materials, is one of the most extensively used technologies for fabricating microcapsules to realize multienzyme system positional assembly extensively.[19] Fabricating polyelectrolyte-doped hollow nanofibers are expected to enable the hollow nanofibers not only to serve as a scaffold for multienzyme immobilization but also to enable precise positional assembly of enzymes in different way via well-developed facile polyelectrolyte LbL technique.

To demonstrate our method is generic, novel polyelectrolyte-doped hollow polyurethane (PU) nanofibers were fabricated for positional assembly of a bienzyme system involving *Candida antarctica* lipase B (CALB) and glucose oxidase (GOD). Lipase catalyzes the reaction of oleic oil with H_2O_2 as oxidant in an oil-aqueous (O/W) biphasic system,[55,56] whereas H_2O_2 will be in situ generated by GOD catalyzed oxidation of glucose as an attempt to avoid rapid deactivation of lipase upon contacting with concentrated of H_2O_2. Epoxy stearate and epoxidized plant oil are both valuable intermediates from which biobased polyols can be generated by a facile ring-opening reaction.[57−60] The polyols are the most important monomer for synthesizing polyurethane materials.[58−60] Moreover, by coupling with the GOD-catalyzed oxidation of glucose, another value-added coproduct glucono-δ-lactone can be obtained, and thus, the

dx.doi.org/10.1021/cs501383j | *ACS Catal.* 2014, 4, 4548−4559

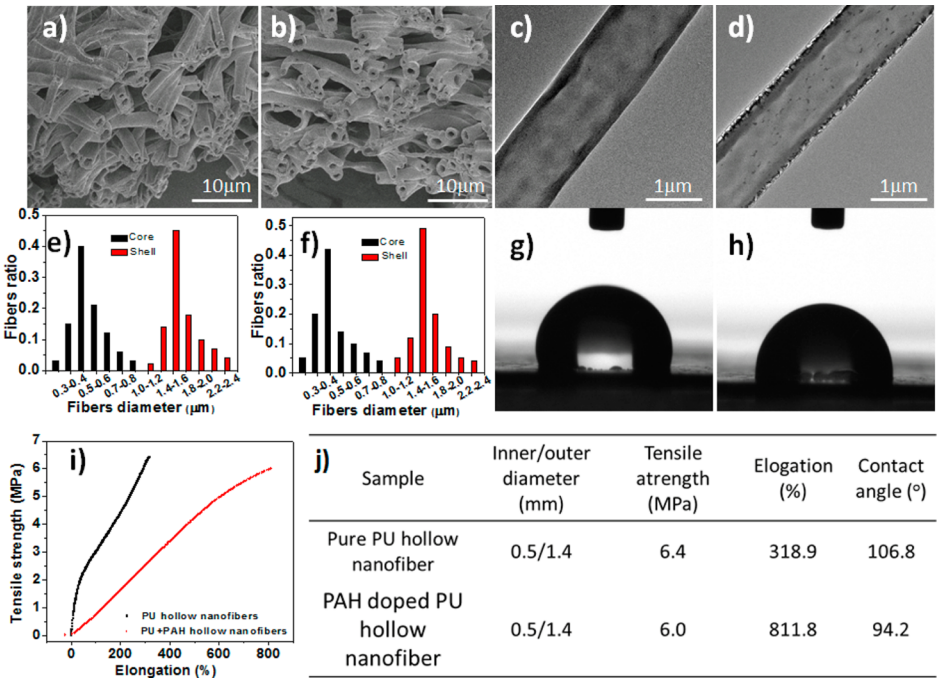

j)

Sample	Inner/outer diameter (mm)	Tensile atrength (MPa)	Elogation (%)	Contact angle (°)
Pure PU hollow nanofiber	0.5/1.4	6.4	318.9	106.8
PAH doped PU hollow nanofiber	0.5/1.4	6.0	811.8	94.2

Figure 1. Characterizations of the PU hollow nanofibers prepared by coaxial electrospinning. (a,b) Cross-sectional SEM images of pure PU hollow nanofibers and PAH doped PU hollow nanofibers produced at core−shell phase solution flow rates: 0.07:0.5 mL/h; (c,d) Shows the corresponding size distribution of the inner and outer diameters of the hollow nanofibers shown in images (a,b); (e,f) TEM images of pure PU hollow nanofibers and PAH doped PU hollow nanofibers; (g,h) Images of an water droplet on pure PU hollow nanofibers membrane and PAH doped PU hollow nanofiber membrane; (i) Tensile strength of pure PU hollow nanofibers membrane and PAH doped PU hollow nanofiber membrane; (j) Summary of the characteristic data.

total economy of the process can be increased. In the present work, the lipase/GOD bienzyme system will be positionally assembled either on the outer surface or inside the lumen of the hollow nanofibers, so that an in-depth investigation on the relationship between positional assembly strategies and the efficiency of multienzyme cascade reaction can be carried out and discussed.

2. RESULTS AND DISCUSSION

2.1. Preparation and Characterization of Cationic Polyelectrolyte Doped PU Hollow Nanofibers. In one of our recent work, hollow PU nanofibers have been successfully prepared via a coaxial electrospinning technique.[54] Here in the present work, to accomplish positional assembly of enzyme, a water-soluble cationic polyelectrolyte, poly(allylamine hydrochloride) (PAH), was doped in to the PU nanofibers by simply dissolving it in the core phase solution of coaxial electrospinning, which was composed of 80% glycerol and 20% water (Scheme 1).

The SEM images of the PU hollow nanofibers and the PAH-doped PU nanofibers showed that the morphology of the hollow nanofibers were not affected by the doping of PAH (Figure 1a,b), both of them exhibited quite uniform size distribution with average inner diameter about 500 nm and outer diameter about 1.4 μm (Figure 1e,f). Compared with the hollow nanofibers without PAH, visible tentacles on both the inner and outer surfaces of the shell of PAH-doped PU hollow nanofibers can be seen in the TEM (Figure 1c,d). Our previous diffusion tests using proteins with different molecular weight as probes have proved that the shell of PU hollow nanofibers have a characteristic molecular weight cutoff (MWCO) about 20 kDa, which means that an encapsulated protein with molecular weight above 20 kDa will not be able to diffuse out from the lumen of the hollow nanofibers.[54] Unlike proteins which are usually in globular shape, PAH is linear. Though the PAH has molecular weight about 40 kDa, exceeding the MWCO of the shell of hollow nanofibers determined using proteins, we speculate that it can still penetrate into the shell of the hollow nanofibers to form tentacles during evaporation of the solvent due to its linear molecular structure. The PAH tentacles therefore would act as binding sites for further anchoring of enzymes either on the outer surface or the inner surface the hollow nanofibers via ion-exchange interactions between enzymes with opposite charges and the ionizable groups of PAH by simply adjusting the pH of the enzyme solution to favorable values.

The presence of ionizable groups on the surface of the PAH doped hollow nanofibers was also supported by its reduced water contact angle. The pure PU hollow nanofiber membrane had a contact angle of 106.8°, while that of the PAH-doped PU hollow nanofiber membrane was reduced to 94.2° (Figure 1g,h). Tensile strength measurement showed that the doping of PAH did not change the tensile strength of the hollow nanofiber membrane much. Therfore, as a result of the linear long-chain PAH doped in the shell of hollow nanofibers, acting as the role of "glue", the elongation at break was significantly increased from 318.9% to 811.8% (Figure 1i), which means the PAH-doped hollow nanofibers were more tenacious than that of pure PU hollow nanofibers, and thus, the PAH-doped hollow nanofibers can be used for much severer reaction conditions than other materials. The major properties of the hollow nanofibers were summarized in Figure 1j.

2.2. Positional Assembly of GOD/CALB Bienzyme System on Hollow Nanofibers. Co-immobilizing enzymes

dx.doi.org/10.1021/cs501383j | ACS Catal. 2014, 4, 4548−4559

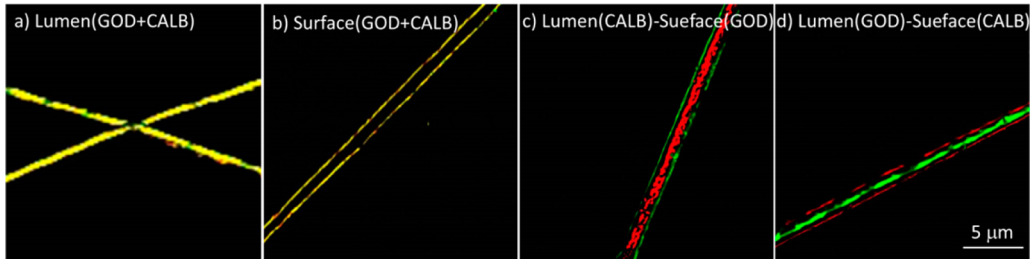

Figure 2. Confocal laser scanning microscope images of the PAH-doped PU hollow nanofibers with positionally assembled GOD/CALB bienzymes. GOD and CALB were labeled by FITC and sulforhodamine 101, respectively, prior to positional assembly.

for performing multistep biotransformations either in cascade or in coupling mode is usually kinetically advantageous over the separately immobilized system because the second enzyme may utilize the product of the first enzyme as substrate directly at very high concentration without need of this product diffusing out from the first biocatalyst and penetrating to the second one.[61,62] On the other hand, this advantage will highly depend on the match of these coimmobilized enzymes in their specific activities and operational stabilities.[61] To realize the advantages of coimmobilization, in the present work, four different coimmobilization strategies were tested by positionally assembling the bienzyme system involving GOD and CALB for cascade reaction to the different locations in hollow nanofibers, which includes lumen (GOD+CALB), surface (GOD+CALB), surface (GOD)-lumen (CALB), and lumen (GOD)-surface (CALB). Placement of enzymes inside the lumen of the hollow nanofibers was easily accomplished by in situ encapsulation during coaxial electrospinning, and the uniformed dispersions of the GOD and CALB inside the lumen of the hollow nanofibers were confirmed by the confocal laser scanning microscope (CLSM) observation (Figure 2a). Due to overlay of the green (FITC-labeled GOD) and red fluorescence (sulforhodamine 101-labeled CALB), strong yellow fluorescence was observed in the merged images.

The doping of cationic polyelectrolyte, PAH, allowed us to assemble the enzymes on the outer surface by ion-exchange interaction between oppositely charged enzymes and the ionizable groups of PAH, which is one of the most widely used mechanisms of LBL technology for preparing multichamber microcapsules and positional assembly multienzyme system due to its mild reaction condition.[21,30] To find the proper condition for enzyme assembly by ion-exchange interaction, zeta-potential of PAH-doped hollow nanofiber membrane was measured over a wide range of pH from 2 to 11. As seen from Figure 3, a significant positive surface zeta-potential was detected for the PAH-doped hollow nanofiber membrane, and the zeta-potential decreased from 250 to 20 mV by increasing the pH of solution from 2 to 12. In contrast, the PU hollow nanofibers membrane without PAH showed a constant zeta-potential of zero. Before zeta-potential measurement, the membrane was immersed in buffer solutions and shaken at least for 10 min. If the PAH was just exposed to the outer surface of the hollow nanofibers instead of penetration across the shell of the hollow nanofibers, most of them would be washed out by shaking and no such significant zeta-potential would be detected. Therefore, this result further confirmed the penetration and protrusion of PAH out of the shell of the hollow nanofibers as we have discussed before, allowing binding of enzymes via ion-exchange interactions over a wide range of pH. Considering the isoelectric points of CALB and GOD were

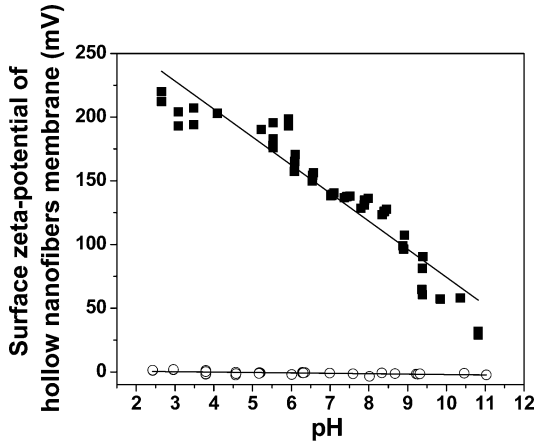

Figure 3. Surface zeta-potential of hollow nanofiber membrane. (○) Pure PU hollow nanofiber membrane. (■) PAH-doped PU hollow nanofiber membrane.

4.9 and 6.0, respectively, they will be negatively charged at pH 7.0 in potassium phosphate buffer (50 mM); therefore, GOD or/and CALB can be quantitatively positionally assembled onto the surface of hollow nanofibers through ion-exchange interaction without need of other cross-linking agents.

The successful coassembly of GOD and CALB on the outer surface of PAH-doped hollow nanofibers through the simple solution-contact procedure was clearly confirmed by CLSM observation shown in Figure 2b. GOD and CALB have molecular weight about 160 kDa and 33 kDa, respectively, which are all above the MWCO the shell of hollow nanofibers, and therefore, the assemblies of these two enzymes are strictly limited to the outer surface of the hollow nanofibers. Through in situ encapsulation and consequent PAH facilitated postassembly on the outer surface of hollow nanofibers, the other two positional assembly strategies, which are surface (GOD)-lumen (CALB) and lumen (GOD)-surface (CALB), were successfully realized, and their corresponding CLSM images are shown in Figure 2c,d.

Loading amounts and activities of CALB and GOD in each of the above-mentioned four bienzyme systems were individually measured, and the results were summarized in Table 1. The activities of enzymes listed in this table represent the results determined using their corresponding standard substrates at well-developed measuring conditions, and the activities of the encapsulated and adsorbed enzyme were determined separately. Specifically, for GOD activity measurement, the rate for glucose oxidation was measured, and for CALB activity measurement, the rate for 4-nitrophenyl acetate hydrolysis was measured. It can be seen that the recovery of activities of GOD and CALB, which were either encapsulated in

dx.doi.org/10.1021/cs501383j | ACS Catal. 2014, 4, 4548−4559

Table 1. Enzyme Loading and Activities of GOD and CALB Which Are Positionally Assembled in PU Hollow Nanofibers through Four Different Strategies[a]

positional assembly strategies	enzyme	enzyme loading (mg-pro/g-fiber)	activity recovery (%)	specific activity (U/mg-enzyme)	gross activity (U/g-fiber)
lumen (GOD+CALB)	GOD	2.17 ± 0.12	83.94 ± 0.71	83.47 ± 0.71	181.14 ± 1.53
	CALB	1.14 ± 0.23	89.26 ± 2.35	14.78 ± 0.39	16.85 ± 1.44
surface (GOD+CALB)	GOD	2.61 ± 0.24	72.43 ± 0.53	72.02 ± 0.53	187.97 ± 1.39
	CALB	1.44 ± 0.32	76.09 ± 2.20	12.60 ± 0.36	18.14 ± 0.52
surface(GOD)-lumen(CALB)	GOD	2.38 ± 0.09	73.03 ± 0.66	72.61 ± 0.63	172.82 ± 1.51
	CALB	1.14 ± 0.17	86.52 ± 0.68	14.33 ± 0.11	16.33 ± 0.13
lumen(GOD)-surface(CALB)	GOD	2.17 ± 0.22	83.73 ± 0.89	83.26 ± 0.88	180.67 ± 1.92
	CALB	1.53 ± 0.31	77.47 ± 0.79	12.83 ± 0.13	19.63 ± 0.60

[a]The activities of the encapsulated and adsorbed enzymes were determined separately. For GOD activity measurement, the rate for glucose oxidation was measured, and for CALB activity measurement, the rate for 4-nitrophenyl acetate hydrolysis was measured.

the lumen or absorbed on the outer surface of hollow nanofibers, were all retained at about 70−80% of their activity in free formation, which can be attributed to the mild condition of immobilization process and the small mass transfer resistance due to the short diffusional distance across the shell of the hollow nanofibers. By adjusting the enzyme concentration and the adsorption time for enzyme binding to the outer surface of the hollow nonofibers, the amount of enzymes in each of the four combinations were controlled approximately the same, so that the effect of the positional assembly strategy on the catalytic efficiency of the bienzyme cascade reaction can be investigated further on the basis of the comparable enzyme dosages.

2.3. Epoxidation Reaction of Oleic Acid by Bienzyme Nanofiber Membrane at O/W Interface. The conversion of oleic acid to epoxy steric acid is a chemo-enzymatic reaction. CALB catalyzes a perhydrolysis from oleic acid to peroxy oleic acid, and then peroxy oleic acid chemically reacts with oleic acid to generate epoxy steric acid.[63−67] For such a reaction, the lipase-catalyzed epoxidation reaction of oleic acid in the presence of H_2O_2 is a typical oil/water (O/W) biphasic reaction system composed of oleic acid dissolved in toluene and the buffer solution with dissolved H_2O_2. In previous reports by other researchers,[55,56,68] the reaction efficiency was usually rather low due to severe interfacial deactivation and the H_2O_2-induced denaturation of enzyme when H_2O_2 was used directly. To avoid the contact of enzyme with concentrated H_2O_2 so that the duration of the enzyme activity can be extended, a hollow nanofibers-based bienzyme system involving GOD and CALB was constructed so that H_2O_2 could be in situ generated by GOD-catalyzed oxidation reaction of glucose.

Another factor limiting the efficiency of O/W biphasic reaction is the availability of enzyme to reactants from both phases across the interface between immiscible chemicals.[69−71] In the O/W biphasic reaction system, the aqueous phase has been traditionally used as a container of the biocatalysts. This oil phase introduces, however, strong mass-transfer limitations for reactants from the organic phase to reach the enzymes, and in most cases, only a small portion of the applied enzyme can be exposed to the interfacial region and is available to substrates.[69] Interface-assembled enzymes that could be simultaneously available to reactants from both phases have been prepared by conjugating enzymes with polymers[69−71] or nanotubes.[72] Both interface-binding enzymes showed significantly improved stability and overall catalytic efficiency for biphasic reactions. But such interfacial enzymes are difficult to be recycled. In this current work, we found, interestingly, that the nanofiber membrane with positionally assembled GOD/CALB bienzyme system through four different strategies were all able to float spontaneously at the interface of the biphasic system consisted of oleic acid dissolved in toluene and the buffer solution of glucose. This phenomenon was speculated to be a result of the proper wettability of nanofiber membrane, whose contact angle is 94°, close to 90°. It has been well-known that for dispersed nanoparticles with a contact angle at O/W interface close to 90°, they tend to spontaneously transfer onto the O/W interface, to self-assembly into thin films,[73−75] or to form a so-called Pickling emulsion by self-assembly to the surface to an emulsion droplet.[37] The spontaneous transfer of continuous hollow nanofiber membrane onto the O/W interface, however, has not been reported so far. Scheme 2 schematically illustrates the bienzyme cascade reaction at the O/W interface, and a picture showing the spontaneous floating of the membrane at the interface is also provided.

Scheme 2. Schematic Illustration of the Epoxidation Reaction of Oleic Acid by GOD/CALB Bienzyme Cascade Reaction at the O/W Interface (Right) and a Picture Showing the Spontaneously Floating Bienzyme Hollow Nanofiber Membrane at the O/W Interface (Left)

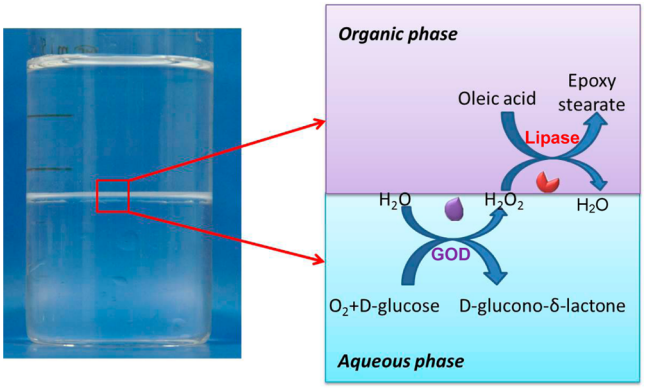

According to the reaction mechanism of this bienzyme cascade reaction, with the oxidation of one mole glucose, one mole of glucono-δ-lactone and one mole of H_2O_2 will be generated, and the latter was then consumed as a substrate for the epoxidation of oleic acid to form epoxy steric acid in the second step via a chemo-enzymatic self-epoxidation mechanism of peroxy oleic acid intermediate. Therefore, from a mass balance point of view, the total generated H_2O_2 (with equal moles to glucono-δ-lactone) should include three terms, the amount of synthesized epoxy steric acid, the peroxy oleic acid intermediate, and the remaining H_2O_2.

dx.doi.org/10.1021/cs501383j | ACS Catal. 2014, 4, 4548−4559

Using these four interfacial bienzyme nanofiber membranes as biocatalysts which were prepared by four different immobilization strategies, the synthesis of product, epoxy stearate, as a function of reaction time is shown in Figure 4, and

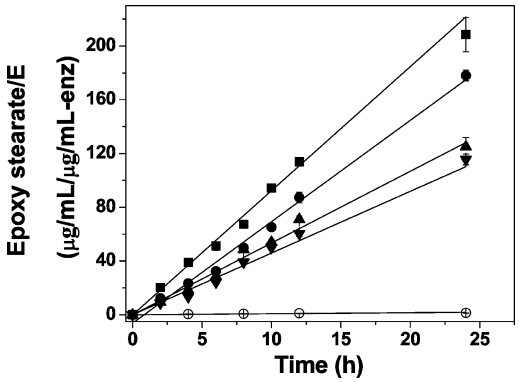

Figure 4. Kinetic curves of oleic acid epoxidation reaction using PU hollow nanofiber-based bienzyme systems. (○) Native GOD+CALB, (●) lumen (GOD+CALB), (▼) surface (GOD+CALB), (▲) surface (GOD)-lumen (CALB), (■) lumen (GOD)-surface (CALB).

the corresponding initial reaction rates are listed in Table 2. Compared to the free bienzyme system, 57.45−114.45 times enhancement in biocatalytic efficiency was attained by using the nanofiber membrane based bienzyme system. Taking the lumen (GOD)-surface (CALB) bienzyme system as an example, Figure 5 demonstrated the time course of changes in measured concentration of glucono-δ-lactone and H_2O_2 in aqueous phase, as well as the decrease in oleic acid concentration and formation of epoxy steric acid in organic phase. It can be seen that the sum of remaining H_2O_2 and the synthesized epoxy steric acid are generally equal to the concentration of glucono-δ-lactone, and the final concentration of epoxy steric acid product is almost identical to the total decrease in oleic acid concentration, indicating a good consistence in mass balance. It should be noted that there was no peroxy oleic acid intermediate detected. In a previous report about the chemo-enzymatic epoxidation of unsaturated carboxylic acids, a very low content of peroxy oleic acid (<2%) was also observed.[65]

Results presented in Figure 4 and Table 2 indicate that all of these four immobilized bienzyme systems have significantly enhanced catalytic efficiencies. The assembly of the nanofiber membrane at the O/W interface is certainly one reason for such enhancement. On the other hand, the immobilization also significantly improved the thermal stability of the enzymes and their resistance to H_2O_2 induced. Result shown in Figure 6 indicates that the free GOD lost about 96.2% of its initial activity after incubation at 40 °C (the temperature for reaction) for 24 h, and both GOD and CALB lost more 80% of their activity after 24 h contacting with 5 wt % H_2O_2. Deactivation of

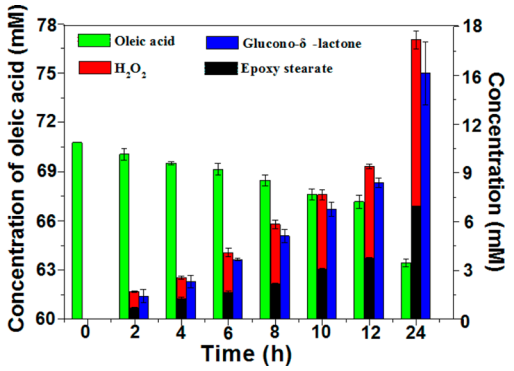

Figure 5. Time course of changes in oleic acid and epoxy steric acid concentration in organic phase, as well as glucono-δ-lactone and H_2O_2 concentration in aqueous phase. The reaction was catalyzed by lumen (GOD)-surface (CALB) bienzyme nanofibers membrane.

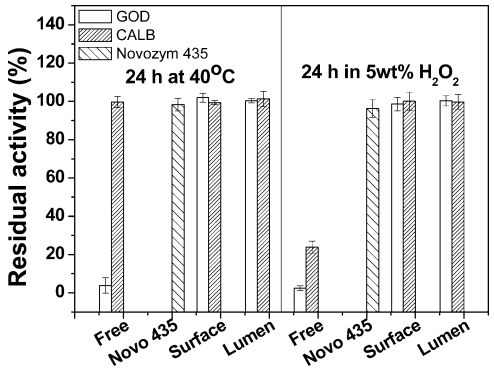

Figure 6. Stabilities of Novozym 435; free and immobilized GOD and CALB at 40 °C; or in the buffer solution containing 5 wt % H_2O_2.

enzymes by H_2O_2 is a very common phenomena, and therefore, H_2O_2 has been considered as a dangerous "liaison" in biocatalysis, because it is a substrate or side product in many enzyme-catalyzed reactions; for example, it is a side product of oxidases, resulting from the reoxidation of FAD with molecular oxygen.[76] At high concentration, H_2O_2 also led to severer deactivation of CALB, such that the fresh enzyme displayed an approximately 50% loss in activity when was used for epoxidation of oleic acid with 30% hydrogen peroxide.[63] In this work, immobilizing the enzymes either on the surface of the hollow nanofibers or inside the lumen of the fiber all led to remarkable improvement in their stabilities that almost 100% of their initial activities were retained after incubation at 40 °C for 24 h, or after 24 h in contact with 5 wt % H_2O_2. The excellent stabilities of the immobilized CALB against thermal and 5 wt % H_2O_2 is even slightly better than that of the commercialized Novozym 435, which is regarded as one of the most powerful industrial immobilized CALB. Such excellent tolerance of the

Table 2. Catalytic Activities and H_2O_2 Utilization Efficiency of Hollow Nanofibers-Based GOD/CALB Bienzyme for Epoxidation of Oleic Acid

bienzyme system	reaction rate (V/[E]) (mg/mL/mg/mL-E)	rate enhancement $(V/[E])_{immobilized}/(V/[E])_{free}$	H_2O_2 utilization efficiency (%)
free (GOD+CALB)	0.080 ± 0.069	1	7.86
lumen (GOD+CALB)	7.54 ± 0.34	94.33 ± 4.27	38.71
surface (GOD+CALB)	4.59 ± 0.56	57.45 ± 7.04	20.55
surface(GOD)-lumen(CALB)	5.34 ± 0.71	66.77 ± 8.92	23.89
lumen(GOD)-surface(CALB)	9.23 ± 0.98	115.47 ± 12.20	55.85

dx.doi.org/10.1021/cs501383j | ACS Catal. 2014, 4, 4548−4559

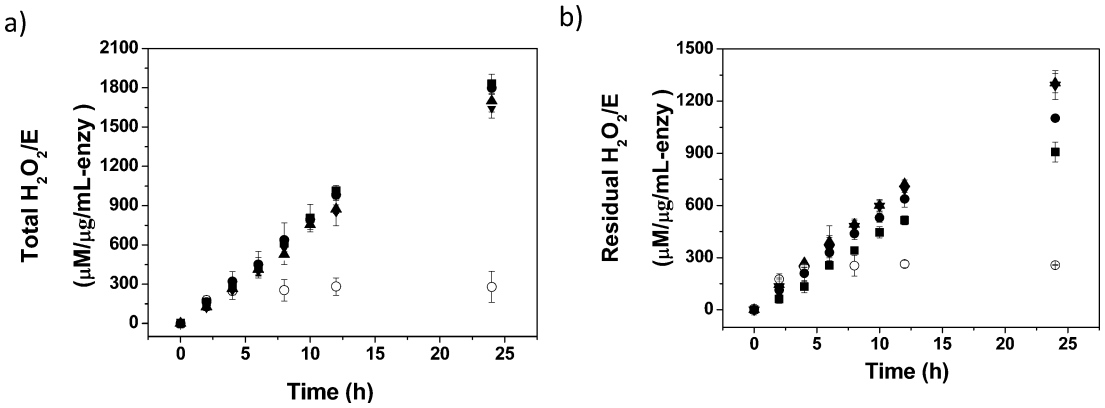

Figure 7. Time course of total generated H_2O_2 in the bienzyme cascade reaction system in the absence of oleic acid (a), and the residual H_2O_2 in the presence of oleic acid. (○) Native GOD+CALB, (●) lumen (GOD+CALB), (▼) surface (GOD+CALB), (▲) surface (GOD)-lumen (CALB), and (■) lumen (GOD)-surface (CALB).

Scheme 3. Schematic Illustrations of the Mechanism of the Bienzyme Cascade Reaction and the Generation and Subsequent Utilization Intermediate H_2O_2 in the Reaction System

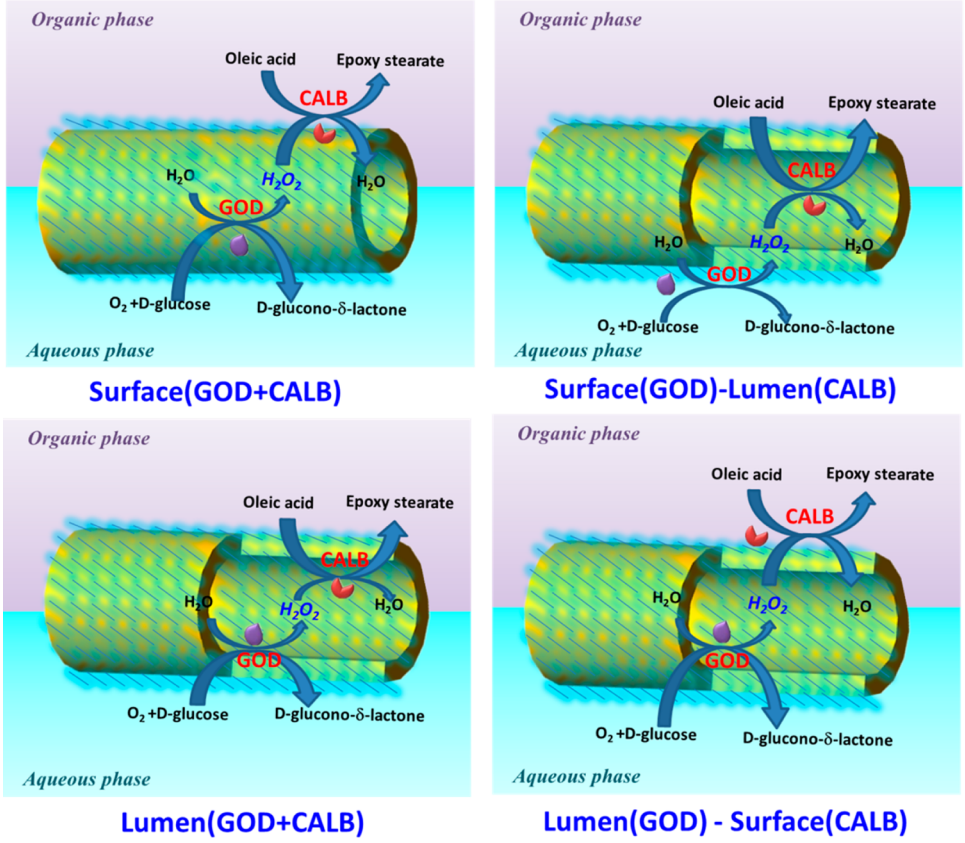

immobilized GOD and CALB against H_2O_2 also enabled us to perform this cascade reaction at excess amount of glucose and higher GOD dosage, and therefore, the limitation of H_2O_2 generating to the overall reaction efficiency could be minimized.

In addition, results listed in Table 2 indicate that the reaction rates of the immobilized bienzyme systems are strongly dependent on the assembly strategies of the two enzymes; the lumen (GOD)-surface (CALB) has the highest activity, whereas activity of the surface (GOD+CALB) is the lowest. Results in Figure 6 have indicated that the effect of position (on surface or inside lumen of the hollow nanofibers) of the enzymes on their intrinsic activities and their stabilities against high temperature (40 °C) and H_2O_2 are very minimal. Therefore, the utilization efficiency of the intermediate product, H_2O_2, in this cascade reaction might be an important factor influencing the total reaction efficiency.

To elucidate the mechanism about the effect of utilization efficiency of H_2O_2 on the overall reaction efficiency, we first analyzed the H_2O_2 formation kinetics in this bienzyme system, but in the absence of oleic acid, substrate of the second step. Figure 7a showed that the total H_2O_2 generated by these four immobilized bienzyme systems were similar, although that of the free system was much lower, mainly due the rapid

dx.doi.org/10.1021/cs501383j | ACS Catal. 2014, 4, 4548−4559

deactivation of free GOD in the biphasic system. With the addition of oleic acid, the generated H_2O_2 will be consumed as oxidant to synthesize epoxy stearate. Figure 7b presents the detected H_2O_2 concentration during the bienzyme cascade reaction. As can be seen, the residual H_2O_2 concentrations follow a decreasing order of surface (GOD+CALB), surface (GOD)-lumen (CALB), lumen (GOD+CALB), and lumen (GOD)-surface (CALB), indicating an increasing order in H_2O_2 utilization efficiency. Because the H_2O_2 was consumed stoichiometrically at molar ratio of 1:1 during the formation of epoxy stearate, therefore, the H_2O_2 utilization efficiency can be calculated by dividing the final concentration of synthesized epoxy stearate to the totally formed H_2O_2 at 24 h in absence of oleic acid (Figure 7a), and the results are listed in Table 2.

The large difference in H_2O_2 utilization efficiency between these four immobilized bienzyme systems may be explained by analyzing the diffusion of H_2O_2 and the consequent capture and utilization of H_2O_2 by CALB. Scheme 3 schematically depicts the detailed mechanism of the cascade reaction catalyzed by each of these four different immobilized bienzyme systems. When GOD was assembled on the outer surface of the hollow nanofibers, the generated intermediate H_2O_2 will diffuse quickly into both the bulk phase of the reaction solution and the lumen phase. The CALB which is assembled on the outer surface will not be able to efficiently capture the H_2O_2 molecule, and therefore, the lowest H_2O_2 utilization efficiency of about 20.55% was obtained in the surface (GOD+CALB) system. Due to the nanoconfining effect, a slightly higher local H_2O_2 concentration inside the lumen might be observed than that in the bulk solution phase, and consequently, a higher H_2O_2 utilization efficiency about 23.89% was observed for the surface (GOD)-lumen (CALB) system. When GOD was encapsulated inside the lumen of the hollow nanofibers, the local concentration of H_2O_2 inside the lumen will be even higher, so that the H_2O_2 utilization efficiency of the lumen (GOD +CALB) system was further improved to 38.71%, and the highest value of 55.85% was achieved for the lumen (GOD)-surface (CALB) system because most of the H_2O_2 can be captured by CABL, when it diffuse across the shell of the hollow nanofibers. Beside effect of H_2O_2 diffusion on its utilization efficiency and the overall catalytic efficiency, the diffusion of epoxy stearate across the nanofiber might also have some effect. For the lumen (GOD)-surface (CALB) system, epoxy stearate was synthesized on the surface of the hollow nanofiber, it can quickly diffuse to the solution, and possible product inhibition on the enzyme could be eliminated. Nevertheless, when CALB was encapsulated inside the lumen of the hollow nanofiber, such as surface (GOD)-lumen (CALB) system, the produced epoxy stearate has to diffuse across the shell of fiber and might accumulate in the lumen.

Results discussed above have clearly demonstrated the significant enhancement in reaction efficiency of this bienzyme cascade reaction by coimmobilizing the two enzymes through different strategies. To further demonstrate the advantages of coimmobilization over separate immobilization, the reaction was also compared with that by GOD and CALB, which were separately immobilized inside the lumen of hollow nanofiber (lumen (GOD)+lumen (CALB)), that by immobilized GOD inside lumen coupling with free CALB (lumen (GOD)+free CALB), as well as that by immobilized GOD inside lumen coupling with Novozym 435 (lumen (GOD)+ Novozym 435). The dosage of the separately immobilized GOD and CALB were all the same as that in the coimmobilized system, although the dosage of Novozym 435 was adjusted to the same activity units as that of CALB in encapsulated formation. Results presented in Figure 8 show that all these three bienzyme system

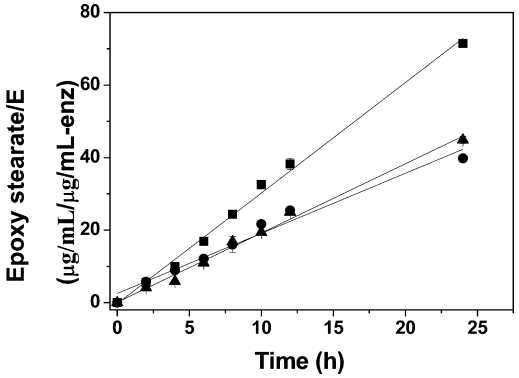

Figure 8. Kinetic curves of oleic acid epoxidation reaction using GOD-Lipase bienzyme system in different formations. (●) Lumen (GOD) + free CALB, (■) lumen (GOD) + lumen (CALB) that are separately immobilized, and (▲) lumen (GOD) + Novozym 435. The dosage Novozym 435 was adjusted to the same unit of hydrolysis activity as that of CALB encapsulated inside lumen of hollow naofibers.

have efficiencies lower than that of the coimmobilized system. Even for the lumen (GOD)+lumen (CALB), which has the highest reaction rate of 2.98 mg/mL/mg/mL−enzyme, that value is still much lower than that of the least efficient coimmobilized system, surface (GOD+CALB), which has reaction rate of 4.59 mg/mL/mg/mL−enzyme) (Table 2). When free CALB and Novozym 435 were applied, they are only distributed in aqueous phase; therefore, the limiting availability of enzymes to reactants from both phases across the interface between immiscible chemicals and the low stability of free CALB led to even lower reaction rate.

2.4. Thermal and Operational Stability of Hollow Nanofibers-Based Bienzyme Systems. The thermal stabilities of the bienzyme system were examined at 60 °C by measuring changes in catalytic efficiency for the cascade reaction after storing the enzymes at this temperature for a different time. It appeared that the hollow nanofibers-based bienzyme systems were remarkably more stable than the native enzymes. Specifically, the native enzymes lost more than 90% of its original activity after being stored at 60 °C for 1 h, while the immobilized bienzyme retained more than 50% of its original activity after a period of 4−9 h (Figure 9). Particularly, the bienzyme systems of lumen (GOD+CALB) and lumen (GOD)-surface (CALB), in which GOD was immobilized inside the lumen, showed the highest thermal stability. This is because the activity of GOD, which is more susceptible to thermal deactivation than CALB, is critical to the overall activity of the bienzyme cascade reaction.

Operational stability of immobilized biocatalyst is an important feature for its potential applications in industry. Figure 10 presents the residual activity of the hollow nanofibers-based bienzyme system versus reusing cycles. By defining the initial reaction rate of the first reaction cycle as 100%, it was found that except for the surface (GOD+CALB) bienzyme system, which retained about 70% of its original activity after 10 cycles of reusing, all of the other three immobilized bienzyme systems could retained as high as 90% of their original activities, indicating an excellent operationally reusability in the biphase system. To better evaluate the

dx.doi.org/10.1021/cs501383j | ACS Catal. 2014, 4, 4548−4559

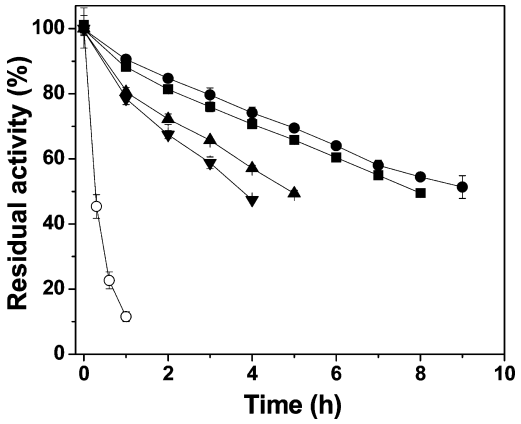

Figure 9. Thermal stability of the bienzyme cascade reaction system at 60 °C. (○) Native GOD+CALB, (●) lumen (GOD+CALB), (▼) surface (GOD+CALB), (▲) surface (GOD)-lumen (CALB), and (■) lumen (GOD)-surface (CALB).

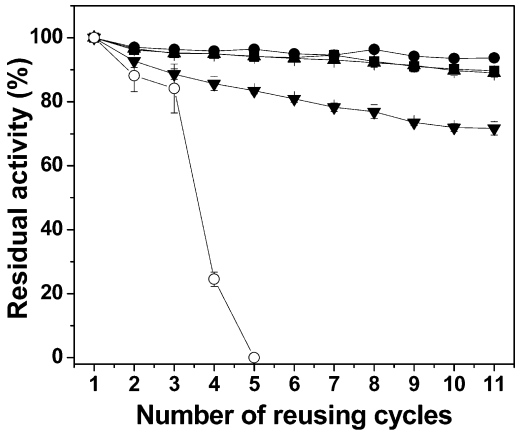

Figure 10. Operational stability of the bienzyme cascade reaction system. Each cycle lasted for 12 h. (●) Lumen (GOD+CALB), (▼) surface (GOD+CALB), (▲) surface (GOD)-lumen (CALB), (■) lumen (GOD)-surface (CALB), and (○) Novozym 435 with added free GOD.

performance of the hollow nanofibers-based bienzymes system, their operational stability was compared with Novozym 435, which is regarded as one of the most powerful industrial immobilized CALB. The reaction was conducted under condition similar to that of the hollow nanofibers-based bienzyme system by adding glucose and free GOD for each cycle of reaction. It can be seen from Figure 8 that after four reusing cycles, the Novozym 435 lost about 80% of its original activity. When H_2O_2 was directly used, the reusability of Novozym 435 was even worse, 88% of its original activity was lost after 2 times utilization.[77] The high efficiency and robust operational activity make the hollow nanofibers-based bienzyme system promising biocatalysts for industrial synthesis of epoxy stearate.

3. CONCLUSION

A novel and generic approach combing the coaxial electrospinning and LBL assembly technologies has been developed for the facile construction of hollow nanofibers-based bienzyme cascade reaction system. Positional assembly of GOD and CALB either inside the lumen or on the outer surface of the hollow nanofibers were realized by in situ encapsulation during coaxial electrospinning process, or through postassembly of enzymes facilitated by its ion-exchange interaction with the doped polyelectrolyte. Meanwhile, these hollow-nanofiber membrane based bienzyme can spontaneously float at the O/W interface, thus making it particularly attractive for biphasic reaction. When this cascade reaction was used for converting oleic acid to epoxy stearate, reaction rates of the nanofiber membrane based bienzyme systems were found to be strongly dependent on the assembly strategies of the two enzymes, and 57.45−114.45 times enhancement in biocatalytic efficiency was attained as compared with that of the free enzymes system. The mechanism accounting for the effect of assembly strategy on the overall efficiency of the cascade reaction was investigated and discussed thoroughly based on an analysis of the utilization efficiency of the intermediate product in the reaction process. Results obtained in this work demonstrates that PAH-doped PU hollow nanofibers provide an ideal scaffold for mimicking natural cell compartmentalization and positional assembly of multienzyme systems for more complicated cascade reactions with high efficiency and easy recyclability, thus promoting and broadening the applications of multienzymatic system in industry, biosensor, biomedical, and many other related research fields.

4. EXPERIMENTAL SECTION

4.1. Materials. Polyurethane A85E (PU) pellet with bulk density about 700 kg/m^3 was supplied by Xiamen Jinyouju Chemical Agent Co. (Xiamen, China). Glucose oxidase (GOD, EC 1.8.1.4), *Candida antarctica* lipase B (CALB, EC 3.1.1.3, a liquid formation with protein concentration about 5.3 mg/mL), Novozym 435 (an immobilized CALB on acylic resin), fluorescein isothiocyanate (FITC), sulforhodamine 101, 2,2′-Azinobis(3-ethylbenzthiazoline-6-sulfonate) (ABTS), oleic acid, were supplied by Sigma. Poly(allylamine hydrochloride) (PAH, molecular weight about 40 kDa) and 4-nitrophenyl acetate were purchased from Alfa Aesar. *N, N*-Dimethylacetylamide (DMAc), glucose, and glycerol were all analytical grade.

4.2. Preparation of Cationic Polyelectrolyte Doped Hollow Nanofibers and Positional Assembly of GOD and CALB. General procedure for fabrication of cationic polyelectrolyte doped hollow nanofibers by coaxial electrospinning: shell solution was prepared by dissolving PU in DMAc to get final polymer concentration of 25 wt %; core solution was prepared by well mixing glycerol (800 μL) with ultrapure water solution (200 μL) containing 20 mg PAH. A spinneret containing two coaxial stainless steel needles was used, with inner and outer diameters of the core nozzles used were 0.42 and 0.72 mm, and that of shell nozzle were 0.92 and 1.28 mm. The core solution and shell solution were fed at 0.07 mL/h and 0.5 mL/h, respectively through two syringe pumps. A positive voltage of 20 kV was applied, and an aluminum sheet was used as the collector at a distance of 30 cm away from the nozzle tip. Electrospinning was carried out at 25 ± 3 °C, humidity 10−15%. The collected scaffolds were placed overnight at room temperature to evaporate residuals solvent.

To positionally assemble the GOD/CALB bienzymatic system in hollow nanofibers, the following four strategies were adopted according to the location of the enzymes. (1) Lumen (GOD+CALB): crude CALB solution was concentration 3-fold by PEG-dialysis, thereafter, concentrated CALB solution (200 μL) with protein concentration about 16.29 mg/mL supplemented with GOD (10 mg, protein content about 62%) was well mixed with glycerol (800 μL) containing PAH

dx.doi.org/10.1021/cs501383j | ACS Catal. 2014, 4, 4548−4559

(20 mg) to form core phase solution of coaxial electrospinning, with which GOD and CALB were in situ encapsulated inside the lumen of hollow nanofibers. (2) Surface (GOD+CALB): a blank hollow nanofiber membrane (about 5 mg) was immersed into potassium phosphate buffer solution (1 mL, 50 mM, pH 7.0) containing GOD (1.0 mg/mL) and CALB (1.0 mg/mL) to immobilized the bienzyme system on the surface of hollow nanofibers via LBL assembly. The incubation was lasted for 0.5 h at 4 °C. At the end of the adsorption, the nanofibers were taken out from the solution and washed several times each with 3 mL of fresh buffer until no protein was detected by Bradford method.[78,79] The enzyme loading amount was calculated via mass balance. (3) Lumen (CALB)-surface (GOD) and (4) lumen (GOD)-surface (CALB): CALB was in situ encapsulated within the hollow nanofibers as described in strategy (1), and GOD was immobilized on the outer surface of the fiber as described in strategy (2) (or vice-visa).

4.3. Characterization. The morphologies of the fibers were characterized by scanning electronic microscopy (SEM, JSM-6700F, JEOL, Japan). To view a cross-section of the hollow nanofibers, the collected nanofibrous membranes were frozen in liquid nitrogen and then cut perpendicularly to expose their hollow structure. To determine the size distribution of the inner and outer diameters of the prepared hollow PU nanofibers, approximately 100 different nanofibers were analyzed from the SEM images. The structures of the fibers were also characterized by transmission electron microscopy (TEM, JEM-2100UHR, JEOL, Japan).

Wettability of the nanofiber membranes was evaluated using a contact angle instrument (DSA100, Kruss, Germany). A droplet of water with controlled volume was deposited on the membrane surface. Shape evolution of the droplet was monitored using a high-speed camera operating at 250 frames per second. Analyses of the drop shape and contact angle measurements were performed using the accompanying software of the instrument. In addition, tensile strength of the nanofiber membranes was also evaluated by dynamic mechanical analyzer (DMA Q800, TA Instrument, U.S.A.).

In order to characterize the distribution of enzymes positional assembly in polyelectrolyte doped hollow nanofibers, GOD was labeled by FITC and CALB was labeled by sulforhodamine 101 prior to positional assembly. The hollow nanofibers with positional assembled enzymes were then characterized by confocal laser scanning microscopy (CLSM) with Leica TCS SP5 microscope (Leica Camera AG, Germany). The laser provided excitation of FITC and sulforhodamine 101 at 488 and 586 nm, and emitted fluorescent light was detected at 545 and 605 nm, respectively. The CLSM images for each nanofiber membranes containing both labeled enzymes were then obtained by merging the fluorescent signal at 545 and 605 nm.

The surface zeta-potential of polyelectrolyte doped hollow nanofibers was measured using a Surpass solid samples zeta-potential analyzer (SurPASS, Austria). The pH of buffer was changed from 2 to 12. Before the measurement, the membrane was cut into a rectangle, immersed into water, and shaken for 10 min.

4.4. Calculation of Encapsulated Enzymes Amount. The total amount of encapsulated substance in the hollow nanofibers prepared at the core−shell solution flow rate of 0.07:0.5 mL h^{-1} was calculated as follows. The total weight of the nanofiber membrane collected after 30 min of stable coelectrospinning was approximately 100 mg. Then, the total volume of electrospun core solution will be 0.035 mL (0.07 mL $h^{-1} \times 0.5$ h). Considering the concentration of substance in the core solution was 10 mg mL^{-1}, for example, in total 0.35 mg of the substance was encapsulated inside the 100 mg membrane sample. Therefore, the amount of substance encapsulated was 0.0035 mg substance per mg nanofiber membrane.

4.5. Enzyme Activity Assay. Activity unit of GOD was defined as the amount of enzyme needed to oxidize 1 μmol glucose to glucose-lactone in 1 min at pH 7.0 and 25 °C. Activity of GOD was determined by measuring the initial oxidation rate of glucose at 25 °C. To potassium phosphate buffer solution (1 mL, 50 mM pH 7.0) containing glucose (30 mg/mL), HRP (5 μg/mL), and ABTS (0.3 mg/mL), free GOD (0.5 μg/mL) or a piece of nanofiber membrane (about 0.5 mg) containing about GOD (1.05 μg) was added to initiate the reaction. The reaction was monitored by measuring the absorbance at 420 nm, A_{420} (ε^{ABTS} =36 mM^{-1} cm^{-1}), continuously for 5 min using a Unico 2800 spectrophotometer. For the activity measurement of nanofibers enzyme, A_{420} was measured at every 30 s after retrieving the fibers with tweezers from the solution.

Activity unit of CALB was defined as the amount of enzyme needed to hydrolyze 1 μmol 4-nitrophenyl acetate to *p*-nitrophenol in 1 min at pH 7.0 and 25 °C. Activity of CALB was determined by measuring the initial hydrolysis rate of 4-nitrophenyl acetate at 25 °C. To potassium phosphate buffer solution (1 mL, 50 mM pH 7.0) containing 4-nitrophenyl acetate (3 mM), free CALB (0.8 μg/mL) or a piece of nanofibrous membrane (about 0.5 mg) containing about CALB (0.6 μg) was added to initiate the reaction. The reaction was monitored by measuring the absorbance at 410 nm, A_{410} ($\varepsilon^{p\text{-nitrophenol}}$ = 24.9 mM^{-1} cm^{-1}), continuously for 5 min using a Unico 2800 spectrophotometer. For the activity measurement of nanofibers enzyme, A_{410} was measured at every 30 s after retrieving the fibers with tweezers from the solution.

4.6. GOD-CALB Bienzyme Cascade Reaction for Epoxidation of Oleic Acid. The bienzyme cascade reaction system consists of two phases due to the difference in solubility of reactants. The aqueous phase (2 mL) consists of glucose (0.2 g/mL) in potassium phosphate buffer solution (50 mmol/L, pH 7.0), and the organic phase consists of oleic acid (20 mg/mL) in toluene (2 mL). The reaction was then initiated by adding free GOD (64 μg/mL) and CALB (32 μg/mL) or nanofiber membranes (about 5 mg) with positional assembled bienzyme system into the two-phase system. The reaction was conducted at 40 °C on an orbital shaker (120 rpm). At time intervals, the organic phase (about 20 μL) was withdrawn, and the amount of formed epoxy stearate product was measured by HPLC (1200 series, Agilent) on a reversed phase Agilent Extend C-18 column (dimensions: 4.6 mm × 150 mm, dp: 5 μm) maintaining at 40 °C. Detection was performed using an evaporative light scattering detector (ELSD, Altech, U.S.A.) equilibrated at 40 °C with an air flow rate of 1.5 mL/min and pressure of 0.5 MPa. Acetonitrile−water (90:10, v/v) was used as mobile phase at a flow rate of 1.0 mL/min.

The H_2O_2 concentration in the aqueous phase was determined by HPLC (1200 series, Agilent) on a reversed phase Agilent Extend C-18 column (dimensions: 4.6 mm × 150 mm, dp: 5 μm) maintained at 30 °C. Detection was performed using an ultraviolet detector (UV, Agilent) at 205 nm. Methanol−water (10:90, v/v) was used as mobile phase at a flow rate of 1.0 mL/min.

dx.doi.org/10.1021/cs501383j | ACS Catal. 2014, 4, 4548−4559

4.7. Thermal Stability and Operational Stability of the Bienzyme System. Thermal stability of the positional assembled bienzyme system was determined by measuring changes in the initial reaction rate of epoxidation reaction of oleic acid after the bienzyme nanofiber membranes were stored at 60 °C for different times. Operational stability of the immobilized bienzyme was examined by measuring the reaction rate of the cascade reactions in biphasic system with the same composition mentioned above. The reactions were run for 12 h before they were stopped by retrieving the nanofiber membrane. After washing the hollow nanofibers-supported bienzymes with buffer solution, fresh substrates including oleic acid and D-glucose were added, and the next reaction measurement was carried out. The reaction rate of the freshly prepared multienzymes system was defined as 100%. The time interval between one reaction cycles to the next round was about 1 h.

AUTHOR INFORMATION

Corresponding Author

*E-mail: spzhang@ipe.ac.cn. Fax: (+86) 10-8254-4958.

Notes

The authors declare no competing financial interest.

ACKNOWLEDGMENTS

The authors thank support from the National Natural Science Foundation of China (Grant Nos. 21376249, 21336010, 20976180, 21106164), and 973 Program (2013CB733604).

REFERENCES

(1) Ricca, E.; Brucher, B.; Schrittwieser, J. H. *Adv. Synth. Catal.* **2011**, *353*, 2239−2262.
(2) Santacoloma, P. A.; Sin, G. r.; Gernaey, K. V.; Woodley, J. M. *Org. Process Res. Dev.* **2010**, *15*, 203−212.
(3) Conrado, R. J.; Varner, J. D.; DeLisa, M. P. *Curr. Opin. Biotechnol.* **2008**, *19*, 492−499.
(4) Koeller, K. M.; Wong, C.-H. *Nature* **2001**, *409*, 232−240.
(5) Schoemaker, H. E.; Mink, D.; Wubbolts, M. G. *Science* **2003**, *299*, 1694−1697.
(6) Bornscheuer, U. T.; Huisman, G. W.; Kazlauskas, R. J.; Lutz, S.; Moore, J. C.; Robins, K. *Nature* **2012**, *485*, 185−194.
(7) Kongjan, P.; Min, B.; Angelidaki, I. *Water Res.* **2009**, *43*, 1414−1424.
(8) Martin del Campo, J. S.; Rollin, J.; Myung, S.; Chun, Y.; Chandrayan, S.; Patino, R.; Adams, M. W. W.; Zhang, Y. H. P. *Angew. Chem., Int. Ed.* **2013**, *52*, 4587−4590.
(9) Rollin, J. A.; Tam, T. K.; Zhang, Y. H. P. *Green Chem.* **2013**, *15*, 1708−1719.
(10) Brady, D.; Jordaan, J. *Biotechnol. Lett.* **2009**, *31*, 1639−1650.
(11) Hernandez, K.; Fernandez-Lafuente, R. *Enzyme Microb. Technol.* **2011**, *48*, 107−122.
(12) Rodrigues, R. C.; Berenguer-Murcia, Á.; Fernandez-Lafuente, R. *Adv. Synth. Catal.* **2011**, *353*, 2216−2238.
(13) Hwang, E. T.; Gu, M. B. *Eng. Life Sci.* **2013**, *13*, 49−61.
(14) Mateo, C.; Palomo, J. M.; Fernandez-Lorente, G.; Guisan, J. M.; Fernandez-Lafuente, R. *Enzyme Microb. Technol.* **2007**, *40*, 1451−1463.
(15) Rodrigues, R. C.; Ortiz, C.; Berenguer-Murcia, A.; Torres, R.; Fernandez-Lafuente, R. *Chem. Soc. Rev.* **2013**, *42*, 6290−6307.
(16) Verma, M. L.; Barrow, C. J.; Puri, M. *Appl. Microbiol. Biotechnol.* **2013**, *97*, 23−39.
(17) Mitragotri, S.; Lahann, J. *Nat. Mater.* **2009**, *8*, 15−23.
(18) van Dongen, S. F.; Nallani, M.; Cornelissen, J. J.; Nolte, R. J.; van Hest, J. C. *Chemistry* **2009**, *15*, 1107−1114.
(19) Peters, R. J. R. W.; Louzao, I.; van Hest, J. C. M. *Chem. Sci.* **2012**, *3*, 335−342.
(20) Kohler, V.; Wilson, Y. M.; Durrenberger, M.; Ghislieri, D.; Churakova, E.; Quinto, T.; Knorr, L.; Haussinger, D.; Hollmann, F.; Turner, N. J.; Ward, T. R. *Nat. Chem.* **2013**, *5*, 93−99.
(21) Marguet, M.; Bonduelle, C.; Lecommandoux, S. *Chem. Soc. Rev.* **2013**, *42*, 512−529.
(22) Szostak, J. W.; Bartel, D. P.; Luisi, P. L. *Nature* **2001**, *409*, 387−390.
(23) Vriezema, D. M.; Garcia, P. M. L.; Sancho Oltra, N.; Hatzakis, N. S.; Kuiper, S. M.; Nolte, R. J. M.; Rowan, A. E.; van Hest, J. C. M. *Angew. Chem.* **2007**, *119*, 7522−7526.
(24) Zhang, Y.; Ruder, W. C.; LeDuc, P. R. *Trends Biotechnol.* **2008**, *26*, 14−20.
(25) Brady, D.; Jordaan, J. *Biotechnol. Lett.* **2009**, *31*, 1639−1650.
(26) Kim, H.; Sun, Q.; Liu, F.; Tsai, S.-L.; Chen, W. *Top. Catal.* **2012**, *55*, 1138−1145.
(27) Schoffelen, S.; van Hest, J. C. M. *Soft Matter* **2012**, *8*, 1736−1746.
(28) Xue, R.; Woodley, J. M. *Bioresour. Technol.* **2012**, *115*, 183−195.
(29) van Dongen, S. F. M.; de Hoog, H.-P. M.; Peters, R. J. R. W.; Nallani, M.; Nolte, R. J. M.; van Hest, J. C. M. *Chem. Rev.* **2009**, *109*, 6212−6274.
(30) Tanner, P.; Egli, S.; Balasubramanian, V.; Onaca, O.; Palivan, C. G.; Meier, W. *FEBS Lett.* **2011**, *585*, 1699−1706.
(31) Duan, L.; He, Q.; Wang, K.; Yan, X.; Cui, Y.; Möhwald, H.; Li, J. *Angew. Chem.* **2007**, *119*, 7126−7130.
(32) Kuiper, S. M.; Nallani, M.; Vriezema, D. M.; Cornelissen, J. J.; van Hest, J. C.; Nolte, R. J.; Rowan, A. E. *Org. Biomol. Chem.* **2008**, *6*, 4315−4318.
(33) Meeuwissen, S. A.; Rioz-Martínez, A.; de Gonzalo, G.; Fraaije, M. W.; Gotor, V.; van Hest, J. C. M. *J. Mater. Chem.* **2011**, *21*, 18923−18926.
(34) Zhang, L.; Shi, J.; Jiang, Z.; Jiang, Y.; Qiao, S.; Li, J.; Wang, R.; Meng, R.; Zhu, Y.; Zheng, Y. *Green Chem.* **2011**, *13*, 300−306.
(35) Patterson, D. P.; Prevelige, P. E.; Douglas, T. *ACS Nano* **2012**, *6*, 5000−5009.
(36) Shi, J.; Wang, X.; Jiang, Z.; Liang, Y.; Zhu, Y.; Zhang, C. *Bioresour. Technol.* **2012**, *118*, 359−366.
(37) Shi, J.; Wang, X.; Zhang, W.; Jiang, Z.; Liang, Y.; Zhu, Y.; Zhang, C. *Adv. Funct. Mater.* **2013**, *23*, 1450−1458.
(38) Delcea, M.; Yashchenok, A.; Videnova, K.; Kreft, O.; Mohwald, H.; Skirtach, A. G. *Macromol. Biosci.* **2010**, *10*, 465−474.
(39) Shum, H. C.; Zhao, Y. J.; Kim, S. H.; Weitz, D. A. *Angew. Chem., Int. Ed. Engl.* **2011**, *50*, 1648−1651.
(40) Kreft, O.; Prevot, M.; Mohwald, H.; Sukhorukov, G. B. *Angew. Chem., Int. Ed. Engl.* **2007**, *46*, 5605−5608.
(41) Delaittre, G.; Reynhout, I. C.; Cornelissen, J. J.; Nolte, R. J. *Chemistry* **2009**, *15*, 12600−12603.
(42) Shi, J.; Zhang, L.; Jiang, Z. *ACS Appl. Mater. Interfaces* **2011**, *3*, 881−889.
(43) Jiang, Y.; Sun, Q.; Zhang, L.; Jiang, Z. *J. Mater. Chem.* **2009**, *19*, 9068−9074.
(44) Stadler, B.; Chandrawati, R.; Price, A. D.; Chong, S. F.; Breheney, K.; Postma, A.; Connal, L. A.; Zelikin, A. N.; Caruso, F. *Angew. Chem., Int. Ed. Engl.* **2009**, *48*, 4359−4362.
(45) Zussman, E.; Yarin, A. L.; Bazilevsky, A. V.; Avrahami, R.; Feldman, M. *Adv. Mater.* **2006**, *18*, 348−353.
(46) Zhao, Y.; Cao, X.; Jiang, L. *J. Am. Chem. Soc.* **2007**, *129*, 764−765.
(47) Zhao, Y.; Jiang, L. *Adv. Mater.* **2009**, *21*, 3621−3638.
(48) Lang, L.; Wu, D.; Xu, Z. *Chemistry* **2012**, *18*, 10661−10668.
(49) Lin, J.; Wang, X.; Ding, B.; Yu, J.; Sun, G.; Wang, M. *Crit. Rev. Solid State Mater. Sci.* **2012**, *37*, 94−114.
(50) Qu, H.; Wei, S.; Guo, Z. *J. Mater. Chem. A* **2013**, *1*, 11513−11528.
(51) Wu, J.; Wang, N.; Zhao, Y.; Jiang, L. *J. Mater. Chem. A* **2013**, *1*, 7290−7305.
(52) Loscertales, I. G.; Barrero, A.; Guerrero, I.; Cortijo, R.; Marquez, M.; Ganan-Calvo, A. M. *Science* **2002**, *295*, 1695−1698.

(53) Loscertales, I. G.; Barrero, A.; Márquez, M.; Spretz, R.; Velarde-Ortiz, R.; Larsen, G. *J. Am. Chem. Soc.* **2004**, *126*, 5376−5377.
(54) Ji, X.; Wang, P.; Su, Z.; Ma, G.; Zhang, S. *J. Mater. Chem. B* **2014**, *2*, 181−190.
(55) Yadav, G. D.; Devi, K. M. *J. Am. Oil Chem. Soc.* **2001**, *78*, 347−351.
(56) Schneider, R. D. S.; Lara, L. R. S.; Bitencourt, T. B.; Nascimento, M. D.; Nunes, M. R. D. *J. Brazil. Chem. Soc.* **2009**, *20*, 1473−1477.
(57) Xu, J.; Jiang, J.; Li, L. *J. Appl. Polym. Sci.* **2012**, *126*, 1377−1384.
(58) Miao, S.; Zhang, S.; Su, Z.; Wang, P. *J. Polym. Sci., Part A: Polym. Chem.* **2010**, *48*, 243−250.
(59) Miao, S. D.; Sun, L. J.; Wang, P.; Liu, R. N.; Su, Z. G.; Zhang, S. P. *Eur. J. Lipid Sci. Technol.* **2012**, *114*, 1165−1174.
(60) Miao, S. D.; Zhang, S. P.; Su, Z. G.; Wang, P. *J. Appl. Polym. Sci.* **2013**, *127*, 1929−1936.
(61) Garcia-Galan, C.; Berenguer-Murcia, Á.; Fernandez-Lafuente, R.; Rodrigues, R. C. *Adv. Synth. Catal.* **2011**, *353*, 2885−2904.
(62) Rocha-Martín, J.; Rivas, B. d. l.; Muñoz, R.; Guisán, J. M.; López-Gallego, F. *ChemCatChem* **2012**, *4*, 1279−1288.
(63) Yadav, G. D.; Devi, K. M. *J. Am. Oil Chem. Soc.* **2001**, *78*, 347−351.
(64) Orellana-Coca, C.; Camocho, S.; Adlercreutz, D.; Mattiasson, B.; Hatti-Kaul, R. *Eur. J. Lipid Sci. Technol.* **2005**, *107*, 864−870.
(65) Warwel, S.; Rüsch gen Klaas, M. *J. Mol. Catal. B: Enzym.* **1995**, *1*, 29−35.
(66) Klaas, M. R. G.; Warwel, S. *J. Am. Oil Chem. Soc.* **1996**, *73*, 1453−1457.
(67) Klaas, M. R.; Warwel, S. *Ind. Crop. Prod.* **1999**, *9*, 125−132.
(68) Törnvall, U.; Orellana-Coca, C.; Hatti-Kaul, R.; Adlercreutz, D. *Enzyme Microb. Technol.* **2007**, *40*, 447−451.
(69) Zhu, G. Y.; Wang, P. *J. Am. Chem. Soc.* **2004**, *126*, 11132−11133.
(70) Zhu, G. Y.; Wang, P. *J. Biotechnol.* **2005**, *117*, 195−202.
(71) Narayanan, R.; Zhu, G. Y.; Wang, P. *J. Biotechnol.* **2007**, *128*, 86−92.
(72) Asuri, P.; Karajanagi, S. S.; Dordick, J. S.; Kane, R. S. *J. Am. Chem. Soc.* **2006**, *128*, 1046−1047.
(73) Binks, B. P. *Curr. Opin. Colloid Interface Sci.* **2002**, *7*, 21−41.
(74) Reincke, F.; Hickey, S. G.; Kegel, W. K.; Vanmaekelbergh, D. *Angew. Chem., Int. Ed.* **2004**, *43*, 458−462.
(75) Duan, H.; Wang, D.; Kurth, D. G.; Mohwald, H. *Angew. Chem., Int. Ed.* **2004**, *43*, 5639−5642.
(76) Hernandez, K.; Berenguer-Murcia, A.; Rodrigues, R. C.; Fernandez-Lafuente, R. *Curr. Org. Chem.* **2012**, *16*, 2652−2672.
(77) da Silva, J. M. R.; Nascimento, M. d. G. *Process Biochem.* **2012**, *47*, 517−522.
(78) Carlsson, N.; Borde, A.; Wolfel, S.; Kerman, B.; Larsson, A. *Anal. Biochem.* **2011**, *411*, 116−121.
(79) Farias, E.; Yasunaga, K. L.; Peixoto, R. V. R.; Fonseca, M. P.; Fontes, W.; Galera, P. D. *Pesqui. Vet. Brasil.* **2013**, *33*, 261−264.